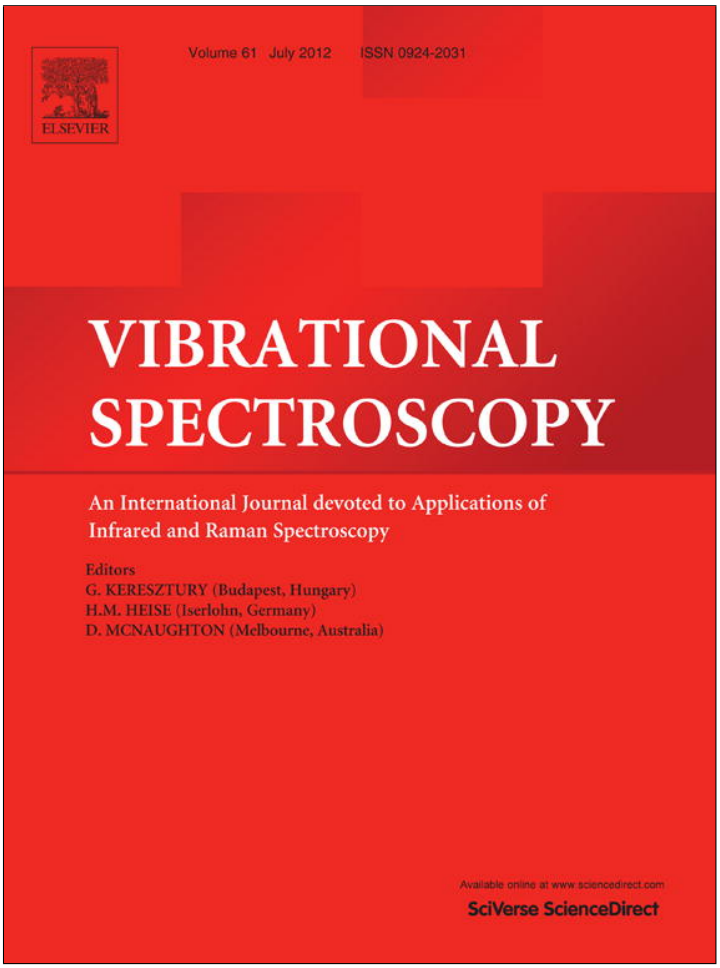

Vibrational Spectroscopy 61 (2012) 156–166

Contents lists available at SciVerse ScienceDirect

Vibrational Spectroscopy

journal homepage: www.elsevier.com/locate/vibspec

Experimental and theoretical study of IR and Raman spectra of tetraoxa[8]circulenes

Valentina A. Minaeva [a], Boris F. Minaev [a,b,*], Gleb V. Baryshnikov [a], Hans Ågren [b], Michael Pittelkow [c]

[a] Bohdan Khmelnytskyy National University, 18031 Cherkasy, Ukraine
[b] Theoretical Chemistry, School of Biotechnology, Royal Institute of Technology, SE-10691 Stockholm, Sweden
[c] Department of Chemistry, University of Copenhagen, Universitetsparken 5, DK-2100 Copenhagen Ø, Denmark

ARTICLE INFO

Article history:
Received 18 November 2011
Received in revised form 30 January 2012
Accepted 2 February 2012
Available online 9 February 2012

Keywords:
Tetraoxa[8]circulenes
DFT calculations
IR spectra
Raman spectra
Symmetry point group
Correlation diagrams, Constituent molecules frequency analysis
Benzene
Naphthalene
Furan

ABSTRACT

The FTIR and Raman spectra of symmetrical derivatives of the tetraoxa[8]circulenes (D_{4h} symmetry) series have been detected and the experimental data have been interpreted by density functional theory (DFT). The equilibrium molecular geometry, harmonic vibrational frequencies, infrared intensities and Raman scattering activities of the studied tetraoxa[8]circulenes have been calculated by the DFT/B3LYP method with the 6–31G(d) basis set using the symmetry constrains. Comparison of the calculated vibrational spectra with the experimental data provides reliable assignments of all observed bands in FTIR and Raman spectra, including the low frequency region. Correlation diagrams with symmetry account of vibrational modes in the studied molecules and their constituents (benzene, naphthalene and furan) have been used and proven very useful in the force field and frequency analysis. The results of quantum-chemical calculations are in excellent agreement with all details of the experimental spectra.

1. Introduction

The family of symmetric tetraoxa[8]circulenes attracts a considerable interest of researchers in recent time as they provide perspective fluorescent material for blue organic light-emitting diodes [1–8].

The first correct structure description of the symmetric tetraoxa[8]circulenes was presented by Erdtman and Högberg in 1968 [9]. In subsequent publications [10–15] Högberg and co-workers continued the study of these compounds by X-ray analysis, UV–visible spectroscopy, mass-spectrometry and ^{1}H NMR-spectroscopy methods, providing important experimental characteristics of the tetraoxa[8]circulene series.

The first *ab initio* quantum-chemical studies of geometrical structure and electronic-orbital properties of symmetric tetraoxa[8]circulenes were published rather recently [1,3]. The UV–visible spectra including absorption and fluorescence was interpreted for first time; the calculated IR spectra of a series of the tetraoxa[8]circulene molecules have also been predicted [3]. It should be noted that the simple [8]circulene (pure hydrocarbon analog of tetraoxa[8]circulene) were studied earlier by quantum-chemical π-approximation [16] and *ab initio* methods [17]. The Sulfur- and selenium-containing analogs of tetraoxa[8]circulenes, such as octathia[8]circulene (empiric formula – $(C_2S)_8$ [5,18–27]), octaselena[8]circulene (empiric formula – $(C_2Se)_8$ [5,23,24]), tetrathiatetraselena[8]circulene (empiric formula – $C_{16}S_4Se_4$ [5,23–26]), decathia[10]circulene (empiric formula – $(C_2S)_{10}$ [27]) have also been investigated in detail by experimental and theoretical methods. Thus, a number of the structural and vibrational spectral properties of the tetraoxa[8]circulene series remain experimentally unknown. This is in contrast to other annulenes and heterocirculenes.

The synthesis of the π-extended tetraoxa[8]circulenes by statistical condensation of 2,3-dialkyl-1,4-benzoquinone with naphthoquinone has been described [1]. By this method we synthesized the series of high-symmetric tetraoxa[8]circulenes, in particular tetraphenylenotetrafuran (4B) and tetranaphthylenotetrafuran (4N). For these compounds (Fig. 1) the FTIR and Raman spectra have been measured, and are presented here. For the assignment of the observed bands in FTIR and Raman spectra we have performed quantum-chemical calculations and analysis of the vibrational spectra at the DFT level.

* Corresponding author. Tel.: +38 0472 376576; fax: +38 0472 354463.
E-mail addresses: bfmin@rambler.ru, boris@theochem.kth.se (B.F. Minaev).

0924-2031/$ – see front matter.
doi:10.1016/j.vibspec.2012.02.005

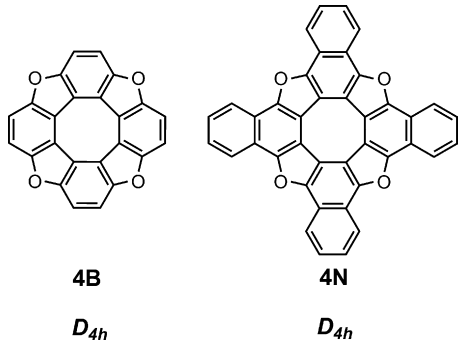

Fig. 1. Structure of symmetrical tetraoxa[8]circulenes.

Comparison of experimental and theoretical vibrational spectra has allowed us to explain the nature of all observed bands in FTIR and Raman spectra. This is unprecedented for these compounds. The knowledge of the nature of the observed bands in vibrational spectra allows a description of the origin of vibronic absorption bands in the UV–visible spectra of tetraoxa[8]circulenes [3]. In the present work it is shown that the observed IR and Raman spectral bands for the 4B and 4N compounds can be assigned on the basis of their comparison with the characteristic bands of free benzene, furan and naphthalene, taking into account the symmetry correlation diagrams.

2. Experimental

The π-extended tetraoxa[8]circulene (4N) was prepared by condensation of naphthoquinone according to our previously published procedure, and was purified by sublimation [1]. The unsubstituted tetraoxa[8]circulene (4B) was prepared by de-*tert*-butylation of the tetra-*tert*-butyl-tetraoxa[8]circulene, according to a literature procedure, and was purified by sublimation [6].

FTIR spectra were recorded on a Bruker Alpha-P FTIR spectrometer (Bruker Optic GmbH, Ettlingen, Germany) equipped with a deuterated triglycine sulfate (DTGS) detector; a temperature-controlled single-bounce diamond attenuated total reflectance (ATR) crystal, and a pressure application device for solid samples.

The Raman spectra were recorded on a BRUKER IFS66 NIR-FT instrument equipped with an FRA106 Raman module. A Nd:YAG laser operating at 1064 nm with an output of 300 mW was used as the exciting source. The detector was a Ge diode cooled to liquid nitrogen temperature.

3. Method of calculation

The structure of the 4B and 4N molecules were optimized at the B3LYP/6–31G(d) [28–30] level of the density functional theory with the control of possible symmetry constrains using the Gaussian 03 package [31]. The vibrational frequencies and the corresponding IR intensities and Raman activities were calculated for the optimized geometry in the framework of the same method. All vibrational mode frequencies were found to be real which indicates that a true minimum on hypersurface of total energy was found. The calculated vibrational frequencies have been scaled in order to provide direct comparison with the experimental spectra. A better agreement between the computed and experimental frequencies can be obtained by using different scale factors for the different optical regions (or types of vibrations): 0.950 for the high frequency region (CH stretchings) and 0.969 for the rest of the spectrum (CC bond stretching in aromatic rings, in plane and out-of-plane deformation vibrations). The scale factors have been calculated as an averaged ratio between the experimentally observed and predicted frequency of all bands in a particular region of IR and Raman spectra of the studied tetraoxa[8]circulenes. It should be noted that similar values of the scale factors are typical and well known for the corresponding spectral regions [32].

The calculated values of Raman activities for the *i*th normal mode (S_i) presented in this work are not identical to the Raman intensities (I_i), though experimental measurements operate with the observed I_i values. Quantum chemical calculations provide Raman activity as a fundamental molecular property determined by response of its electronic shell [31]. Although it is clear that the calculated Raman activities and the measured relative Raman intensities are not readily comparable [33,34], the similarities in the corresponding observed and calculated spectral traces are still recognizable (the relative intensities above 1000 cm^{-1} should gradually decrease, while those below 1000 cm^{-1} gradually increase compared to the Raman scattering activities).

The calculated IR and Raman spectra of the studied tetraoxa[8]circulenes were constructed with the SWizard program [35] (half-width is 15 cm^{-1}, the Lorenz distribution function). The detailed vibrational assignment of fundamental modes were performed on the ground of the calculated vibrational modes animation with GaussView 5.0 program [31], which gives a visual presentation of vibrational modes, and with account of comparison between calculated and experimental IR frequencies of benzene, furan and naphthalene molecules.

For the description of symmetrical tetraoxa[8]circulene vibrational spectra we used a continuous numbering of all the normal modes which was given in accordance with increasing vibration frequencies.

4. Results and discussion

4.1. Molecular geometry of symmetrical tetraoxa[8]circulene molecules

The optimized molecular structures with the numeration of atoms and the choice of axes are shown in Fig. 2. Some selected optimized geometrical parameters are also presented in Fig. 2. The benzene rings in the 4B molecule are marked by I–IV numeration; the condensed benzene rings forming naphthalene fragments in the 4N molecule are marked by I(a, b)–IV(a, b) numeration (Fig. 2). The geometry parameters, presented in Fig. 2, are in a good agreement with the X-ray diffraction data for the related *tert*-butyl substituted tetraoxa[8]circulene (4B) molecule [6], with one exception for the CO bonds in furan rings (calc.: 1.385 Å against exp.: 1.392 Å and 1.402 Å).

Since, in the IR spectral analysis, we compare vibrational spectra of tetraoxa[8]circulene molecules with the corresponding vibrational spectra of benzene, furan and naphthalene molecules we have to consider the analogical structural parameters of the chosen prototype molecules (benzene, furan and naphthalene). This comparison is also presented in Fig. 2. The analysis indicates that the condensed benzene and furan rings in the 4B molecule are 'swelling' compared to the free benzene and furan rings. All the calculated CC bond lengths in the condensed benzene rings of the 4B compound are increased as compared to the CC bond lengths in the free benzene molecule (1.391 Å). On the contrary, the CH bond lengths are shorter in the 4B molecule (1.084 Å) as compared to benzene (1.095 Å). The $C^3C^\alpha C^\beta$ valence angle is larger by 2.6°, and other angles are smaller (Fig. 1) as compared to those in the benzene molecule. In the condensed furan rings the CO bond lengths are longer by 0.021 Å, and the $C^\alpha C^\beta$ ($C^{\alpha'}C^{\beta'}$) bonds are longer by 0.039 Å in comparison with the free furan molecule (Fig. 2). The $C^\beta C^{\beta'}$ bond length and the $C^\alpha OC^{\alpha'}$ valence angles are slightly smaller (0.005 Å) and by 0.7°, respectively. The furan and benzene rings are forming the united extended π-system in the 4B molecule. Therefore

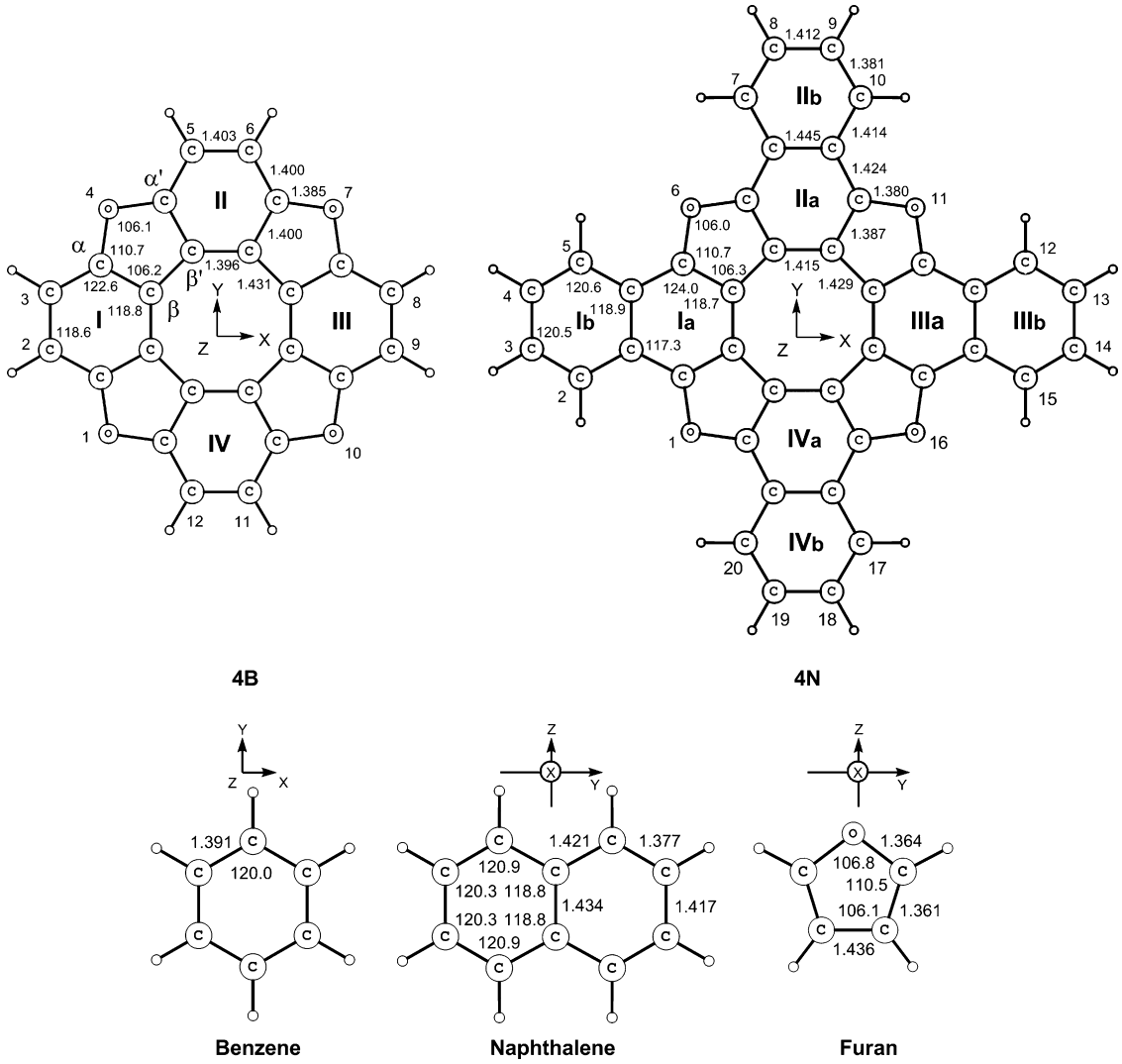

Fig. 2. Selected geometrical parameters, systematic numeration of atoms and choice of axes for the studied symmetrical tetraoxa[8]circulene, benzene, furan and naphthalene molecules.

the 4B molecule has the planar structure characteristic of the D_{4h} symmetry point group.

One can note that for the pure hydrocarbon [8]circulene it could be logically possible to assume also the existence of the united extended π-system. But in contrast to the family of tetraoxa[8]circulenes the former pure hydrocarbon has non-planar structure and belongs to the D_{2d} symmetry point group. Thus, the existence of the furans is crucial for the planarity of tetraoxa[8]circulenes. The characteristic feature of the both types of [8]circulenes is the presence of the entire cyclooctatetraene-type circle; in accord with the Hückel rule $(4n+2)$ the cyclooctatetraene is not aromatic, but provides a formal anti-aromatic structure $(4n, n=2)$.

The all-naphthalene 4N structure is a symmetric analog of the parent 4B molecule (Figs. 1 and 2). In both molecules the geometry parameters of furans are almost identical; a minor exclusion represents the $C^{\alpha}C^{\beta}$ and $C^{\alpha'}C^{\beta'}$ bond lengths which are shortened by 0.013 Å in the 4N molecule (Fig. 2). The presence of four naphthalene fragments in the 4N molecule leads to equalizing of the CC bond lengths in the entire cyclooctatetraene circle, which differ by only 0.014 Å, whereas in 4B they differ by 0.035 Å. The naphthalene fragments inside the 4N molecule exhibit negligible deformation in comparison with free naphthalene; this is a sequence of condensation of the Ia–IVa rings with the furan fragments and an overall involvement of naphthalenes into the united extended π-system.

Accounting for the fact that the benzene, furan and naphthalene rings in the studied tetraoxa[8]circulenes are involved in the united extended π-system one can expect an existence in the vibrational spectra of these compounds not only individual characteristic modes of these constituents but also an occurrence of the mixed vibrations and corresponding IR bands.

4.2. IR and Raman spectra of the 4B tetraoxa[8]circulene molecule

The 4B tetraoxa[8]circulene molecule, consisting of 36 atoms, has 102 normal modes of vibrations. According to the D_{4h} symmetry point group they can be classified as follows: 34 E_u, 9 A_{1g}, 8 A_{2g}, 9 B_{2g}, 9 B_{1g} – in-plane vibrations; 16 E_g, 4 A_{1u}, 4 A_{2u}, 4 B_{2u}, 5 B_{1u} – out-of-plane vibrations. In the IR spectrum only E_u, and A_{2u} are allowed; in the Raman spectrum the A_{1g}, E_g, B_{2g}, and B_{1g} vibrations are allowed in the electric dipole approximation. All allowed vibrational modes in the IR and Raman spectra of the 4B tetraoxa[8]circulene molecule are presented and assigned in Table 2. For the degenerate vibrations the number of second paired modes is given in parenthesis. For the spectral region 1800–400 cm^{-1} (finger print) the experimental and

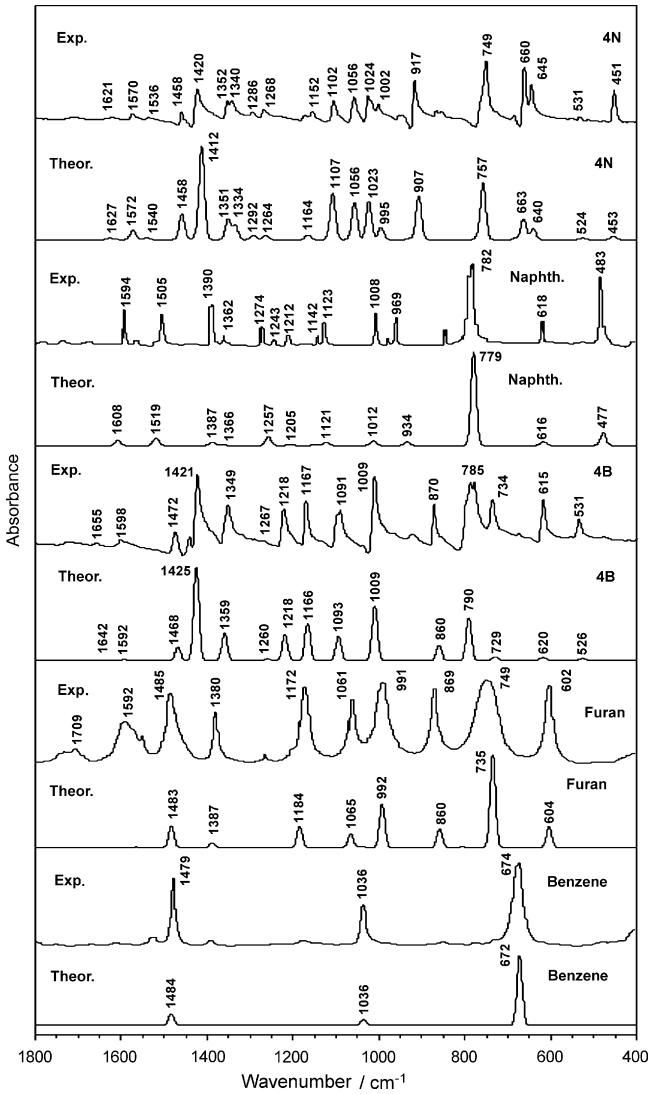

Fig. 3. Calculated and experimental IR spectra for symmetrical tetraoxa[8]circulene, benzene, furan and naphthalene molecules.

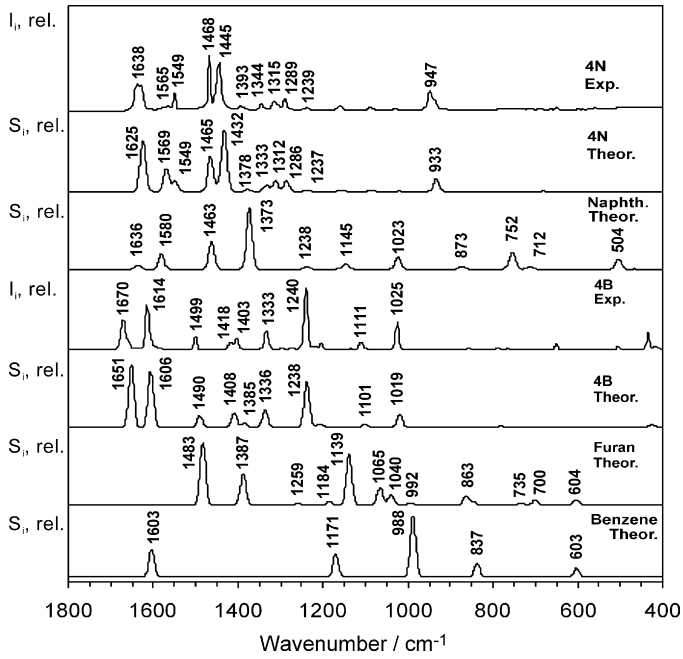

Fig. 4. Calculated and experimental Raman spectra for symmetrical tetraoxa[8]circulene, benzene, furan and naphthalene molecules. The relative Raman intensity (I_i, rel.) and relative Raman activity (S_i, rel.) are given for the ordinate axis labeling the experimentally measured and calculated Raman spectra, respectively.

calculated IR spectra of all studied molecules are presented in Fig. 3, the Raman spectra – in Fig. 4.

4.2.1. CH vibrations

The carbon–hydrogen vibrations in aromatic compounds can be found in the range 3080–3030 cm^{-1} (CH stretching), 1225–950 cm^{-1} (in-plane CH deformations), and below 900 cm^{-1} (out-of-plane CH deformation vibrations) [36,37].

4.2.1.1. The CH stretching vibrations, ν(CH). The CH stretching vibrations of the condensed benzene rings in the 4B tetraoxa[8]circulene molecule according to our DFT calculation have to be observed in the narrow region 3073–3061 cm^{-1} (ν_{102}–ν_{96}). The calculated 3072 cm^{-1} mode are symmetric CH stretching vibrations, 3061 cm^{-1} – are asymmetric. In the experimental IR spectrum of the 4B molecule they are observed as a weak wide band at 3090–3056 cm^{-1}.

In the calculated IR spectrum of benzene (the D_{6h} symmetry point group) the analogous symmetric and asymmetric CH vibrations are predicted at the identical frequency (3041 cm^{-1}) with the identical IR absorption intensity (51.9 km/mole). The observed IR spectrum of benzene in gas phase exhibits an intense band at 3064 cm^{-1} [38] and at 3036 cm^{-1} in a condensed phase [39]. Thus we can explain a small high frequency shift of benzene CH stretching vibrations, their splitting and intensity quenching in the parent 4B tetraoxa[8]circulene molecule.

In the Raman spectrum of the 4B molecule a set of vibrational modes ν_{102}, ν_{99}, ν_{98} with close-lying frequencies create a strong band at 3073 cm^{-1} (exp.: 3078, 3051 cm^{-1}). The degenerate stretching vibrations of the E_u symmetry in IR spectrum and γ(CH) vibrations of the E_g symmetry in Raman spectrum occur simultaneously in two opposite rings of the 4B molecule, whereas the A_{1g}, B_{2g}, B_{1g} vibrations being active in Raman spectrum occur simultaneously in all rings. The largest activity with in Raman spectrum (986.4 Å/amu) exhibits the totally symmetric CH stretching mode ν_{102}.

4.2.1.2. The planar CCH deformation vibrations, δ(CH). The planar deformation vibrations, δ(CH), are calculated in the range 1260–1009 cm^{-1} (Table 2). As a rule, these vibrations are mixed with ν(CO) and/or with the rings stretchings. In the calculated IR spectrum of 4B (Fig. 3) the δ(CH) vibrations are predicted at 1260, 1218, 1166, 1093 and 1009 cm^{-1}. Almost all these bands have a medium intensity of IR absorption. In the experimental IR spectrum the corresponding bands are observed at 1267, 1218, 1167, 1091 and 1009 cm^{-1} demonstrating a perfect agreement with the theory (Fig. 3). In the calculated Raman spectrum of the 4B molecule (Fig. 4) the δ(CH) vibrations provide very intense band ν_{71} at 1238 cm^{-1} and two weak bands 1101 (ν_{62}) and 1019 cm^{-1} (ν_{58}). In the latter mode the δ(CH) deformation vibrations are mixed in phase with the breathings of benzenes and furans; in out-of-phase combination they are mixed with the breathings of the eight-membered ring.

In the calculated IR spectrum of benzene the δ(CH) vibrational band is predicted at 1036 cm^{-1} (the E_{1u} mode) which coincides with the experimental value [38,39]; the corresponding band in the 4B molecule is found at 1093 cm^{-1} ($\nu_{61(60)}$), thus demonstrating a strong frequency shift. In Raman spectrum of benzene this type of vibrations is predicted at 1171 cm^{-1} (the E_{2g} mode;

experiment: 1178 cm^{-1} [38]). This corresponds to the B_{1g} (ν_{62}) mode in Raman spectrum of 4B. This vibrational mode at 1101 cm^{-1} (ν_{62}) belongs only to the planar CH deformations and does not contain any contributions from other vibrations. Thus it can be definitely connected with the corresponding δ(CH) band in benzene (1171 cm^{-1}) demonstrating a strong low-frequency shift of about 70 cm^{-1}.

4.2.1.3. Out-of-plane deformation vibrations, γ(CH). The strong band ν_{46} at 790 cm^{-1} (exp: 785 cm^{-1}) and the weak band ν_{30} at 620 cm^{-1} (exp: 615 cm^{-1}) in IR spectrum of 4B both belong to the out-of-plane deformation vibrations, of the A_{2u} symmetry. The γ(CH) vibration in the benzene molecule according to our calculations occurs at 672 cm^{-1} (exp: 674 cm^{-1} [38,39]) and provides the most intense absorption band in IR spectrum of benzene. The band ν_{30} at 620 cm^{-1} includes not only the out-of-plane CH deformation but also the COC fragments of furans. The corresponding out-of-plane HCOCH vibrations of the B_1 symmetry in the IR spectrum of furan are calculated at 604 cm^{-1} (exp: 615 cm^{-1} [39]).

In the Raman spectrum of 4B the out-of-plane deformation vibrations of the E_g symmetry are calculated in the range 897–637 cm^{-1} (Table 2). The modes $\nu_{53(52)}$ and $\nu_{32(31)}$ have low activity and cannot be observed in the Raman spectrum of the 4B molecule.

We conclude that the calculated CH vibration frequencies (stretching and deformation) in the 4B tetraoxa[8]circulene molecule are in a good agreement with the measured spectra and many of them show considerable shifts in comparison with the spectra of benzene and furan as a result of condensation of these simple aromatic rings into the tetraoxa[8]circulene extended π-system.

4.2.2. Ring vibrations

4.2.2.1. The benzene fragments CC stretching vibrations. The IR bands of the skeleton vibrations of the aromatic CC bonds are usually observed in the region 1650–1430 cm^{-1} [36,37]. Since the permanent dipole moment of the benzene molecule is equal to zero, only asymmetric CC vibrations are allowed in its IR spectrum (E_{1u} vibrations, calc: 1484 cm^{-1}; gas phase IR spectrum: 1484 cm^{-1} [38], in condensed phase: 1479 cm^{-1} [39], Fig. 3). In the IR spectrum of the 4B molecule which contains four condensed benzene rings these vibrations constitute four doubly degenerate vibrational modes of the E_u symmetry with the calculated frequencies 1642 ($\nu_{93(92)}$), 1592 ($\nu_{88(87)}$), 1468 ($\nu_{85(84)}$) and 1425 cm^{-1} ($\nu_{82(81)}$). In the experimental IR spectrum of 4B we observe a very strong band at 1421 cm^{-1} and well distinguished absorption at 1472 cm^{-1}, both being correspond to the latter two modes of the asymmetric ν_{as}(CC) type. To the former two modes in the experimental IR spectrum corresponds very weak bands of symmetric CC vibrations at 1655 and 1598 cm^{-1} (Fig. 3). One should stress that none of the skeleton vibrations of the benzene fragments (Fig. 5a) which are allowed in IR spectrum of 4B molecule (Fig. 5b–e) do not exactly correspond by their form to the benzene ν(CC) vibrational modes (Fig. 5g and h), since they are mixed with other displacements. The band at 1468 cm^{-1} of the ν_{as}(CC) type has essential contributions of the CC vibrations in furan.

The mode $\nu_{76(75)}$ (calc.: 1359 cm^{-1}, exp.: 1349 cm^{-1}) of the medium IR intensity belong to the skeleton vibrations of the benzene rings, which include subsequent alternations of the CC bonds stretching and compression of large amplitude (Kekule vibrations, Fig. 5f). In IR and Raman spectra of benzene vibrations of this type (B_{2u}), calculated at 1313 cm^{-1}, are symmetry forbidden and have never been observed. The clear appearance of this peak in the IR spectrum of 4B (Fig. 3) is an interesting manifestation of mutual atomic influence and common conjugation effect. In the

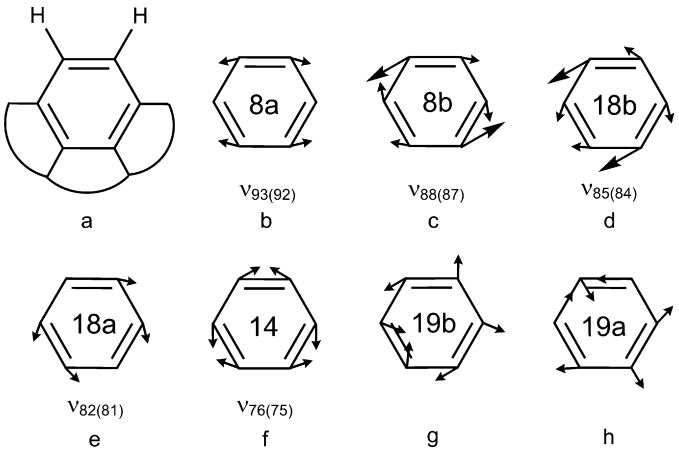

Fig. 5. Calculated forms of the IR-active carbon–carbon skeletal scattering vibrations of the benzene fragment (a) in 4B (b–e) and benzene (g and h) molecules and vibration by the Kekule type in 4B molecule (f). The labels in the center of the ring correspond to Wilson vibrational modes numbering of the free benzene molecule [40].

Raman spectrum of the 4B molecule eight corresponding modes are allowed: three modes ν_s(CC), three modes ν_{as}(CC) and two pure Kekule vibrations.

Symmetric CC vibrations of the B_{2g} and B_{1g} type (modes ν_{91} and ν_{90}, respectively, calculated at 1606 and 1604 cm^{-1} in the 4B molecule) are very similar to the 1603 cm^{-1} vibration band in the Raman spectrum of benzene (ν_{16} according to Herzberg's numeration [38]). The ν_{91} mode contains appreciable contribution of the δ(COC) vibrations of the furan rings, which explain a small frequency shift. The most intense peak in the Raman spectrum of 4B molecule (Fig. 4) is the totally symmetric A_{1g} mode ν_{94} at 1651 cm^{-1} (exp.: 1670 cm^{-1}). Asymmetric CC vibrations are less intense; these are bands with low intensity at 1490 and 1408 cm^{-1} in the calculated Raman spectrum of 4B (Fig. 4). The latter band is produced by two overlapping modes: ν_{79} (B_{2g}) and ν_{78} (A_{1g}). The mode ν_{78} corresponds to the Kekule vibrations. A similar type of vibration can be attributed to the ν_{74} (B_{1g}) mode calculated at 1336 cm^{-1}, which is absent in IR spectrum, but is observe clearly in Raman scattering (Fig. 4).

The appearance of numerous CC vibrations of benzene fragments in the IR and Raman spectra of the 4B molecule, which are strictly forbidden at the D_{6h} symmetry restriction of pure benzene, illustrates important fundamental properties of the united π-system of the tetraoxa[8]circulene. The non zero intensity of the corresponding bands in the IR absorption and Raman scattering of 4B provides clear assignment of the force field and correct interpretation of all the vibrational modes. They occur more informative than the small structural changes, presented in Fig. 2, in respect to comprehensive understanding of electronic structure peculiarities in the large family of tetraoxa[8]circulene compounds.

4.2.2.2. Furan related vibrations. Vibration of the $C^{\beta}C^{\beta'}$ bond of the A_1 symmetry in free furan (C_{2v} point group) which is active in both IR and Raman spectra occurs at 1380 cm^{-1} (calc.: 1387 cm^{-1}). This vibration is split in to four corresponding modes in IR spectrum of the 4B molecule (A_{1g} modes ν_{94}, ν_{86}, ν_{78} and ν_{71}). Symmetric vibrations of the $C^{\alpha}C^{\beta}$ bonds of the A_1 symmetry are allowed in both IR and Raman spectra of furan and calculated in free furan molecule at 1483 cm^{-1} (exp.: 1485 cm^{-1}, Fig. 3) can be seen only in the Raman scattering of the 4B molecule (A_{1g} mode ν_{86}, calc.: 1490 cm^{-1}, exp.: 1499 cm^{-1}); they have some δ(COC) contribution and do not provide any large frequency shift upon the rings condensation.

In the experimental IR spectrum of 4B there are four CO vibrational modes of the E_u symmetry at 1267, 1218, 1167 and 1009 cm^{-1}, which agree well with the theoretical prediction (Table 2). All these modes contain contribution of δ(CH) vibrations in benzene fragments. Both symmetric and asymmetric vibrations of the CO bonds are accompanied by stretching of the opposite pair of benzene rings.

The very weak band at 1267 cm^{-1} in the IR spectrum of 4B is assigned to the ν_{as}(CO) ($\nu_{73(72)}$, calc.: 1260 cm^{-1}, Fig. 3). In the IR spectrum of furan it is also very weak and exhibits no shift, which is in agreement with the calculation. The rest of ν(CO) bands are mixed with the in-plane δ(CH) vibrations and show moderate intensity in the IR spectrum of 4B (Fig. 3). In the Raman spectrum we predicted a strong band at 1238 cm^{-1} which is attributed to the δ(CH) vibrations being mixed with the symmetric stretch of the CO bonds; all nuclear movements proceed in phase (A_{1g} symmetry). The red wing of this bond is formed by two modes ν_{68} and ν_{66}, the former one is ν_s(CO) and occurs at 1214 cm^{-1}, the latter mode is ν_{as}(CO) at 1202 cm^{-1}, which includes also out-of-phase stretchings of I–IV benzene fragments.

4.2.2.3. Deformation vibrations of the rings. Planar skeleton deformations of benzene, furan and octatetraene rings are observed in breathing and stretchings of the rings. Many of them are mixed with other types of vibrations and already have been discussed above. But there are some particular modes which should be mentioned. First of all these are modes $\nu_{50(49)}$ responsible for the band at 860 cm^{-1} of moderate intensity in the calculated IR spectrum of 4B (exp.: 870 cm^{-1}) which belong to furan breathing. In experimental spectra their intensity are much higher than the theory predict (Fig. 3). It should be noted, that the ring breathing is a symmetric movement of all nuclei in the ring; the ring stretching includes also simultaneous movements but not necessary symmetrical for all deformations.

The totally symmetrical benzene ring breathing (A_{1g} vibration) is allowed in the Raman scattering, but is forbidden in IR absorption. It is predicted at 988 cm^{-1} and is observed in the Raman spectrum of benzene at 993 cm^{-1} [39]. In the 4B molecule the benzene breathings are mixed out-of-phase with the octatetraene ring and are observed in the Raman spectrum at 1019 cm^{-1} (exp.: 1025 cm^{-1}). It also contains the δ(CH) vibrations.

We have predicted in-phase breathing of all rings at 425 cm^{-1} (exp.: 434 cm^{-1}); this mode is the most active in low-frequency region of the Raman spectrum of the 4B molecule (S_i = 40.9 Å^4/amu).

Symmetric and asymmetric in-plane deformations of benzene fragments produce very weak absorption bands in the calculated IR spectrum of the 4B molecule at 729 and 526 cm^{-1}, but in the experimental spectrum these bands are more intense (exp.: 734 and 531 cm^{-1}, Fig. 3).

Benzene rings deformation of similar type predicted in the Raman spectrum at 774, 642 and 498 cm^{-1}, are also very weak (Fig. 4), but now in reasonable agreement with experiment (Table 2). It is interesting to note that symmetric deformations of the octatetraene ring can be detected in Raman scattering of 4B species in low-frequency region; calculations predict a weak signal at 297 cm^{-1} (S_i = 23.3 Å^4/amu); asymmetric in-plane deformations of the cyclooctatetraene at 256 cm^{-1} are less active (Table 2).

In general we can conclude that our DFT calculations explain all visible features in experimental spectra and predict some new ones in low-frequency region.

4.3. IR and Raman spectra of the 4N tetraoxa[8]circulene molecule

In the 4N molecule there are 174 normal modes. According to the vibrational selection rules under D_{4h} point group symmetry, they can be classified as follows:

$$\Gamma_{vib} = 15A_{1g}(R) + 14A_{2g} + 15B_{1g}(R) + 15B_{2g}(R) + 58E_u(IR) + 7A_{2u}(IR) + 8B_{1u} + 7B_{2u} + 7A_{1u} + 28E_g(R).$$

All Raman and IR active vibrational modes of the 4N molecule are presented in Table 3.

4.3.1. CH vibrations

4.3.1.1. CH stretching. The calculated carbon–hydrogen stretching vibrations in naphthalene fragments occur in the range 3058–3031 cm^{-1}. In the IR spectrum of 4N the CH stretching vibrations produce occasionally degenerate modes; these are symmetric vibrations $\nu_{173(172)}$ (calc.: 3058 cm^{-1}) and asymmetric CH stretching vibrations $\nu_{169(168)}$ (calc.: 3053 cm^{-1}), $\nu_{165(164)}$ (calc.: 3042 cm^{-1}) and $\nu_{161(160)}$ (calc.: 3031 cm^{-1}, Table 3). All these modes with the half-width of 15 cm^{-1} produce one weak absorption band in the experimental IR spectrum of the 4N molecule with a maximum at 3040 cm^{-1}. In the naphthalene IR spectrum (D_{2h} symmetry point group, *yz* is a molecular σ_h plane) the symmetric CH stretching vibrations of the B_{2u} symmetry are calculated at 3047 cm^{-1} (I = 59.4 km/mole); the asymmetric CH stretching in naphthalene are also slightly shifted and provide together one line with the similar maximum.

In the Raman spectrum of naphthalene the ν_s(CH) and ν_{as}(CH) stretching vibrations of the A_g symmetry are calculated at 3048 and 3024 cm^{-1}, respectively; the ν_{as}(CH) vibrations of the B_{3g} symmetry we predict at 3035 and 3017 cm^{-1}. In the Raman scattering spectrum of the 4N compound each naphthalene ν(CH) stretching mode of the A_g symmetry is split into two, A_{1g} and B_{1g} modes, which are occasionally degenerate by frequency. The ν_{as}(CH) vibrations of the B_{3g} symmetry of the naphthalene D_{2h} group in the Raman spectrum of 4N are also split into degenerate modes of the A_{2g} and B_{2g} symmetry in the D_{4h} point group. It should be noted that the A_{2g} mode is forbidden in Raman (and IR) spectra. As a result, the totally symmetrical A_{1g} mode ν_{174} and the B_{1g} (ν_{171}) mode, which belong to symmetrical CH stretching, together with the B_{2g} (ν_{170}) mode of the asymmetrical ν_{as}(CH) vibrations (Table 3) provide in the Raman spectrum of 4N a medium intensity band with a maximum at 3058 cm^{-1} (exp.: 3061 cm^{-1}) at the same time the modes A_{1g} (ν_{166}) and B_{2g} (ν_{162}) form a right shoulder of this band.

Thus in the Raman spectrum of the 4N molecule, as well as in its IR absorption spectrum, one can see the slight frequency increase of CH stretching vibrations as a result of geometry parameters change upon condensation of the naphthalene rings.

4.3.1.2. The planar CCH deformation vibrations, δ(CH). In-plane CCH deformation vibrations, δ(CH), are calculated in the range 1286–1023 cm^{-1} (Table 3). The deformation E_u mode ($\nu_{118(117)}$) of 4N calculated at 1264 cm^{-1} (exp.: 1268 cm^{-1}) corresponds to the B_{1u} (ν_{31}) vibration in the IR spectrum of naphthalene (calc.: 1257 cm^{-1}). This weak, but prominent band in Fig. 3, is accompanied by a series of weak signals, such as E_u mode ($\nu_{113(112)}$) of 4N calculated at 1164 cm^{-1} (exp.: 1172 cm^{-1}), which corresponds to the B_{1u} (ν_{25}) vibration in IR spectrum of naphthalene (calc.: 1121 cm^{-1}; exp.: 1123 cm^{-1}; Fig. 3, Table 3). The A_{1g} mode ν_{119}, calc.: 1286 cm^{-1}, determined by Ia–IVa rings breathing, includes also a large contribution of the δ(CH) vibrations.

From the δ(CH) group one has to mention strong bands calculated at 1107 cm^{-1} ($\nu_{105(104)}$; exp.: 1102 cm^{-1}) of E_u symmetry of 4N (Fig. 3) and δ(CH) band at 1023 cm^{-1} ($\nu_{97(96)}$), which transfers into the B_{2u} (ν_{23}) vibration in the IR spectrum of naphthalene (calc.: 1012 cm^{-1}; exp.: 1008 cm^{-1}; Fig. 3). In total, the planar CCH deformation vibrations in 4N are shifted about 10 cm^{-1} to higher frequency comparing with the corresponding IR spectrum of

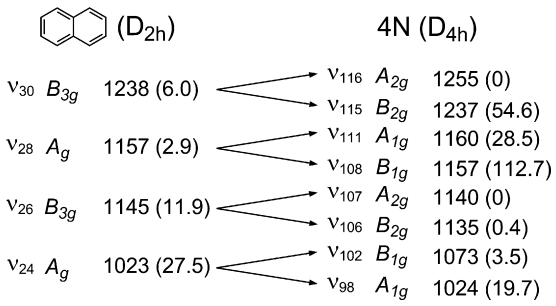

Fig. 6. The splitting of the four Raman-active δ(CH) vibrational modes of naphthalene to eight vibrational modes in 4N molecule Raman spectrum. (The numbers in parentheses after the wavenumber values correspond to Raman activities.)

naphthalene. The stronger force constants of the in-plane CCH bending potential in 4N is a result of increased π-delocalization of the whole ring and CC bonds alternation in naphthalene fragments (Fig. 2).

The strong IR band $\nu_{105(104)}$ (calc.: 1107 cm^{-1}) of E_u symmetry in 4N includes also ν_{as}(CO) vibrations (Table 3) connected with asymmetric planar deformations of the naphthalene fragments Ia, IIIa or IIa, IVa. It has no direct analogy in naphthalene IR spectrum.

Correlation diagram for Raman-active deformation vibrations δ(CH) of naphthalene and the 4N molecule is presented in Fig. 6. Each naphthalene mode is doubly split, often providing some enhancement of the Raman scattering in the 4N molecule. The low-active mode ν_{30} of naphthalene (B_{3g} symmetry) is widely split in the Raman spectrum of 4N into two modes: the forbidden A_{2g} vibration and very active B_{2g} vibration. Another prominent transformation occurs for the mode ν_{28} of naphthalene (A_g symmetry) which provides very weak signal; in the Raman spectrum of 4N it is split into two active modes. A strong enhancement of the Raman scattering at 1157 cm^{-1} upon condensation of naphthalene rings into the 4N structure up to 112.7 Å^4/amu (Table 3) is quite prominent in the observed spectrum (see supplementary material).

4.3.1.3. Out-of-plane planar vibrations, γ(CH). The non planar CH deformation vibrations, γ(CH), in naphthalene fragments of the 4N molecule are observed in the 959-453 cm^{-1} region. Each γ(CH) mode of the B_{3u} symmetry in naphthalene (ν_{20} and ν_6) are split in the IR spectrum of 4N into two mode of the A_{2u} and B_{2u} symmetry. The former A_{2u} modes provide weak IR bands at 927 and 453 (B_{2u} is forbidden in D_{4h} point group).

The ν_{14} (B_{3u} symmetry) mode of the naphthalene molecule (in-phase γ(CH) vibrations; calc.: 779 cm^{-1}) is split in the IR spectrum of 4N into four modes, which provide absorption band of moderate intensity at 660 cm^{-1} (calc.: 663 cm^{-1}) and a strong band observed at 749 cm^{-1} (calc.: 757 cm^{-1}); other modes are not active. Such a strong splitting and large low-frequency shift upon condensation of naphthalene rings into the 4N structure is rather unexpected for the

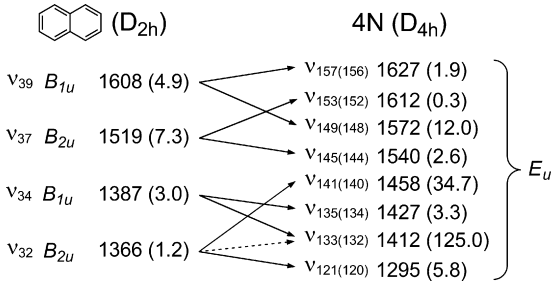

Fig. 7. The splitting of the four IR-active ν(CC) vibrational modes of naphthalene to eight doubly degenerate vibrational modes in 4N molecule IR spectrum. (The numbers in parentheses after the wavenumber values correspond to IR intensities.)

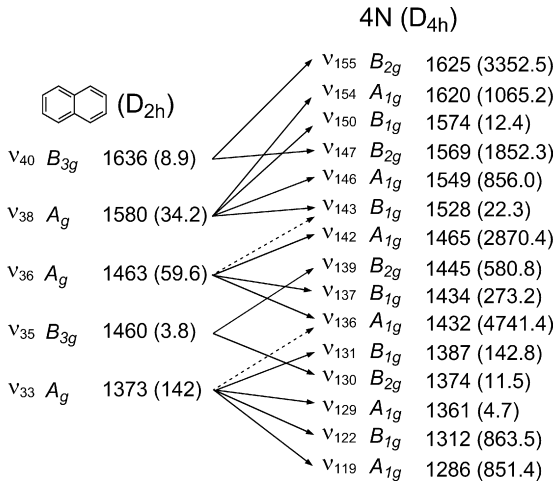

Fig. 8. The splitting of the five Raman-active ν(CC) vibrational modes of naphthalene to fifteen vibrational modes in 4N molecule Raman spectrum. (The numbers in parentheses after the wavenumber values correspond to Raman activities.)

out-of-plane CH vibrations, but it is well reproduced in theory. Similar in-phase γ(CH) vibration in IR spectrum of the 4B molecule was observed at 785 cm^{-1} (calc.: 790 cm^{-1}). The behavior of the non planar CH vibrations upon condensation into the tetraoxa[8]circulene is the most intriguing finding of our study.

In the Raman spectrum of the 4N molecule the allowed doubly degenerate γ(CH) vibrations of E_g symmetry are very weak and therefore are not seen in Fig. 4.

4.3.2. Ring vibrations

4.3.2.1. The naphthalene fragments CC stretching vibrations. The CC stretching vibrations in naphthalene fragments of the 4N molecule are observed in the IR spectrum at lower frequencies in comparison with analogous vibrations of benzene rings in the 4B molecule. The CC stretching vibrations in 4N constitute 16 modes (eight doubly degenerate vibrations of E_u symmetry); they are formed by splitting of the B_{2u} and B_{1u} modes of naphthalene (Fig. 7). In the IR spectrum of 4N these CC stretching modes provide in most cases the very weak bands (Fig. 3); their calculated frequencies are in a perfect agreement with experiment. The most prominent band at 1458 cm^{-1} has essential contribution from the furan $\nu(C^{\beta}C^{\beta'})$ vibrations, being similar to the corresponding band (1468 cm^{-1}) in IR spectrum of the 4B molecule.

Table 1
Correlation between vibrational modes symmetry in the D_{4h}, D_{2h}, and C_{2v} point groups.

D_{4h}	D_{2h}		C_{2v}
xy	xy[a]	yz[a]	yz
E_g	B_{2g}	B_{2g}	B_1
E_g	B_{3g}	B_{1g}	A_2
A_{1g}	A_g	A_g	A_1
A_{2g}	B_{1g}	B_{3g}	B_2
B_{1g}	A_g	A_g	A_1
B_{2g}	B_{1g}	B_{3g}	B_2
E_u	B_{2u}	B_{2u}	B_2
E_u	B_{3u}	B_{1u}	A_1
A_{1u}	A_u	A_u	A_2
A_{2u}	B_{1u}	B_{3u}	B_1
B_{1u}	A_u	A_u	A_2
B_{2u}	B_{1u}	B_{3u}	B_1

[a] For the D_{2h} point group two variants (xy and yz) of the "horizontal" plane of symmetry (σ_h) are given in order to compare with the σ_h choice in 4B and 4N molecules.

Table 2
Calculated frequencies, IR and Raman intensities and corresponding experimental data and assignment of vibrational modes for 4B molecule.

No.	Sym.	Fre.	I_{IR}	S_i	Exp.	Assignment
ν_{102}	A_{1g}	3073	–	986.4	3078 (R)	CH str., s., iph.
$\nu_{101(100)}$	E_u	3072	14.1	–	3090 (IR)	CH str., s., I, III oph. (II, IV oph.)
ν_{99}	B_{1g}	3072	–	356.6	3078 (R)	CH str., s., I, III and II, IV oph.
ν_{98}	B_{2g}	3061	–	354.7	3051 (R)	CH str., as., I, III oph., II, IV oph.
$\nu_{97(96)}$	E_u	3061	0.4	–	3056 (IR)	CH str., as., I, III (II, IV) iph.
ν_{94}	A_{1g}	1651	–	989.8	1670 (R)	CC str. I–IV and $C^{\beta}C^{\beta'}$ str., oph.
$\nu_{93(92)}$	E_u	1642	1.0	–	1655 (IR)	CC str., s., I, III oph. (II, IV oph.)
ν_{91}	B_{2g}	1606	–	876.5	1614 (R)	CC str., s., COC bend.
ν_{90}	B_{1g}	1604	–	8.4		CC str., s., $C^{\alpha}C^{\beta}$ and $C^{\alpha'}C^{\beta'}$ str., as.
$\nu_{88(87)}$	E_u	1592	1.9	–	1598 (IR)	CC str., s., II, IV oph. (I, III oph.)
ν_{86}	A_{1g}	1490	–	178.4	1499 (R)	$C^{\alpha}C^{\beta}$ and $C^{\alpha'}C^{\beta'}$ str., s., $C^{\beta}C^{\beta'}$ str., COC bend.
$\nu_{85(84)}$	E_u	1468	22.3	–	1472 (IR)	CC str., as., I, III (II, IV), $C^{\beta}C^{\beta'}$ str.
$\nu_{82(81)}$	E_u	1425	156.0	–	1421 (IR)	CC str., as., I, III (II, IV)
ν_{80}	B_{1g}	1417	–	0.3		CC str., as., I, III and II, IV oph.
ν_{79}	B_{2g}	1409	–	115.0	1418 (R)	CC str., as., I, II and III, IV oph., $C^{\alpha}C^{\beta}$ and $C^{\alpha'}C^{\beta'}$ str., s.
ν_{78}	A_{1g}	1408	–	124.4	1418 (R)	CC str., as., Kekule, $C^{\beta}C^{\beta'}$ str., COC bend.
ν_{77}	B_{2g}	1385	–	76.2	1403 (R)	$C^{\beta}C^{\beta'}$ str., I–IV def., as., ip.
$\nu_{76(75)}$	E_u	1359	45.8	–	1349 (IR)	CC str., as., Kekule, II, IV (I, III)
ν_{74}	B_{1g}	1336	–	264.4	1333 (R)	CC str., as., Kekule, I, III and II, IV, oph.
$\nu_{73(72)}$	E_u	1260	3.2	–	1267 (IR)	CO str., as., str., II, IV oph. (I, III), CH ip. bend.
ν_{71}	A_{1g}	1238	–	718.6	1240 (R)	CH ip., bend., CO, $C^{\beta}C^{\beta'}$ str., I–IV and ct. str., oph.
$\nu_{70(69)}$	E_u	1218	44.0	–	1218 (IR)	CH ip. bend., CO str., s. I, III oph. (II, IV)
ν_{68}	B_{2g}	1214	–	34.0	1219 (R)	CH ip. bend., CO str., s.
ν_{66}	B_{1g}	1202	–	33.1	1203 (R)	CH ip. bend., CO str., as., I, III and II, IV str., oph.
$\nu_{65(64)}$	E_u	1166	62.5	–	1167 (IR)	CH ip. bend., CO str., s., I, III oph. (II, IV)
ν_{63}	A_{1g}	1132	–	0.7		CH ip. bend., iph.
ν_{62}	B_{1g}	1101	–	51.8	1111 (R)	CH ip. bend., I, III and II, IV oph.
$\nu_{61(60)}$	E_u	1093	40.2	–	1091 (IR)	CH ip. bend., II, IV oph. (I, III)
ν_{58}	A_{1g}	1019	–	208.3	1025 (R)	I–IV, fu and ct. bre., oph., CH ip. bend.
$\nu_{57(56)}$	E_u	1009	91.7	–	1009 (IR)	CH ip. bend., CO str., as., I, III (II, IV)
ν_{55}	B_{2g}	982	–	0.1		I–IV, def. ip.
$\nu_{53(52)}$	E_g	897	–	0.3		CH op. bend., as., II, IV (I, III)
$\nu_{50(49)}$	E_u	860	25.0	–	870 (IR)	fu., I, III oph., bre. (fu., II, IV)
ν_{48}	B_{1g}	855	–	11.9	857 (R)	I, III and II, IV str., oph., ct. str., CO str. as.
ν_{46}	A_{2u}	790	143.8	–	785 (IR)	CH op., bend., I–IV iph.
$\nu_{45(44)}$	E_g	785	–	6.9	787 (R)	CH op. bend., s., I, III (II, IV) oph.
ν_{42}	B_{2g}	774	–	10.7	765 (R)	I–IV ip., as., def., COC bend.
$\nu_{41(40)}$	E_u	729	6.7	–	734 (IR)	I, III (II, IV) oph., s. def, II, IV (I, III) as. def.
$\nu_{38(37)}$	E_g	692	–	0.2		II, IV (I, III) def., op., iph.
ν_{34}	A_{1g}	642	–	12.5	650 (R)	I–IV def., ip., iph., COC bend., iph.
$\nu_{32(31)}$	E_g	637	–	0.3		fu. def. op., CH op. bend., II, IV (I, III) oph.
ν_{30}	A_{2u}	620	6.8	–	615 (IR)	CH, COC and ct. op., bend., oph.
$\nu_{29(28)}$	E_u	613	2.6	–		II, IV def, oph. (I, III)
$\nu_{26(25)}$	E_u	526	4.1	–	531 (IR)	II, IV def., as. (I, III)
ν_{24}	B_{1g}	498	–	9.3	504 (R)	I, III and II, IV def., s., oph., ct. def.
$\nu_{23(22)}$	E_g	496	–	0.5		II, IV (I, III) def., op., iph.
ν_{19}	B_{2g}	468	–	1.4	476 (R)	I–IV sw., ip.
ν_{17}	A_{1g}	425	–	40.9	434 (R)	fu., I–IV, ct. bre., iph.
$\nu_{16(15)}$	E_g	404	–	5.7	417 (R)	fu., I, III (II, IV) def., op.
$\nu_{14(13)}$	E_u	363	3.0	–		I, III (II, IV) sw., II, IV (I, III) def., oph.
ν_{10}	B_{1g}	297	–	23.3	304 (R)	ct. def., s., ip.
ν_9	A_{2u}	273	7.0	–		Skeleton def., op.
ν_8	B_{2g}	256	–	1.7		ct. def., as., ip.
$\nu_{7(6)}$	E_g	251	–	4.7	261 (R)	I–IV, fu., ct. def. op.
$\nu_{5(4)}$	E_g	181	–	4.2	193 (R)	II, IV (I, III) def., op., oph.
ν_1	A_{2u}	79	2.1	–		Skeleton waving

No., mode number; Sym., symmetry species; Fre., frequency (cm^{-1}); I_{IR}, IR intensity (km/mol); S_i, Raman activity ($Å^4$/amu); Exp., experimental; def., deformation; bre., breathing; s., symmetric; as., asymmetric; iph., in-phase; oph., out-of-phase; I, II, III, IV, benzene ring numbers (see Fig. 2); bend., bending; sw., swinging; fu., furan; ct., cyclooctateraene ring, str., stretching; ip., in-plane; op., out-of-plane.

The most intense modes $\nu_{133(132)}$ in the calculated IR spectrum of the 4N molecule include the Kekule vibrations of the "a" rings in two opposite naphthalene fragments (Ia and IIIa), which correspond to ν_{32} of the free naphthalene molecule; they have contribution of the asymmetric vibrations of the CC bonds in two other opposite rings (IIa and IVa). The Kekule vibrations in the "b" rings of two opposite naphthalene fragments are observed in the modes $\nu_{121(120)}$. Vibrational modes $\nu_{128(127)}$ and $\nu_{125(124)}$ forming the moderate doublet band at 1351 and 1334 cm^{-1} in the calculated IR spectrum of the 4N species (experiment: 1352 and 1340 cm^{-1}) belong to the mixed vibrations of furan ν(CO) and ν(CC) naphthalene rings.

In Raman spectrum of the 4N molecule the valence ν(CC) vibrations of naphthalene rings are very active and produce the scattering bands at 1625, 1569, 1465, 1432, 1378 and 1312 cm^{-1} (experiment: 1638, 1565, 1468, 1445, 1393 and 1315 cm^{-1}). They are formed by splitting of each corresponding mode of the B_{3g} symmetry in naphthalene into two modes of the B_{2g} symmetry in the 4N species and each the A_g mode – into vibrations of the A_{1g} and B_{1g} symmetry (Fig. 8). We have to remember that the modes ν_{158}, ν_{151}, ν_{138} and ν_{126} of the A_{2g} symmetry are forbidden in Raman scattering. The modes B_{2g} ν_{147} and A_{1g} ν_{136} have essential contributions of the COC deformation vibrations.

Table 3
Calculated frequencies, IR and Raman intensities and corresponding experimental data and assignment of vibrational modes for 4N molecule.

Num.	Sym.	Fre.	I_{IR}	S_i	Exp.	Assignment
ν_{174}	A_{1g}	3058	–	1441.0	3061 (R)	CH str., s., iph.
$\nu_{173(172)}$	E_u	3058	63.1	–	3040 (IR)	CH str., s., II, IV (I, III) oph.
ν_{171}	B_{1g}	3058	–	83.9		CH str., s., I, III and II, IV oph.
ν_{170}	B_{2g}	3053	–	343.6		CH str., as., I, III oph., II, IV oph.
$\nu_{169(168)}$	E_u	3053	25.4	–		CH str., as., II, IV (I, III) iph.
ν_{166}	A_{1g}	3042	–	247.9		CH str., as., I, III oph.
$\nu_{165(164)}$	E_u	3042	24.2	–		CH str., as., II, IV (I, III) oph.
ν_{163}	B_{1g}	3042	–	607.8		CH str., as., I, III and II, IV oph.
ν_{162}	B_{2g}	3031	–	225.2		CH str., as., I, III oph., II, IV oph.
$\nu_{161(160)}$	E_u	3031	1.4	–		CH str., as., II, IV (I, III) iph.
$\nu_{157(156)}$	E_u	1627	1.9	–	1621 (IR)	I, III (II, IV), CC str., s., iph.
ν_{155}	B_{2g}	1625	–	3352.5	1638 (R)	I, III and II, IV CC str., s., oph.
ν_{154}	A_{1g}	1620	–	1065.2	1630 (R)	$C^{\beta}C^{\beta'}$ str., I, III and II, IV CC str., s., oph.
$\nu_{153(152)}$	E_u	1612	0.3	–		CC str., s., I and III (II and IV) oph.
ν_{150}	B_{1g}	1574	–	12.4		CC str., s., I, III and II, IV oph.
$\nu_{149(148)}$	E_u	1572	12.0	–	1570 (IR)	CC str., s., IIa, IVa (Ia, IIIa) iph., CC str., as., IIb, IVb (Ib, IIIb)
ν_{147}	B_{2g}	1569	–	1852.3	1565 (R)	CC str., Ia–IVa, s., Ib–IVb, as., COC ip. bend.
ν_{146}	A_{1g}	1549	–	856.0	1549 (R)	CC str., Ib–IVb, as., iph., $C^{\beta}C^{\beta'}$ str.
$\nu_{145(144)}$	E_u	1540	2.6	–	1536 (IR)	CC str., as., I, III (II, IV)
ν_{143}	B_{1g}	1528	–	22.3	1530 (R)	CC str., as., I, III and II, IV oph.
ν_{142}	A_{1g}	1465	–	2870.4	1468 (R)	CC str., as., I–IV iph., $C^{\beta}C^{\beta'}$ str., $C^{\alpha}C^{\beta}$, $C^{\alpha'}C^{\beta'}$ str., s.
$\nu_{141(140)}$	E_u	1458	34.7	–	1458 (IR)	CC str., as., I and III (II and IV) oph., $C^{\beta}C^{\beta'}$ str.
ν_{139}	B_{2g}	1445	–	580.8		$C^{\beta}C^{\beta'}$ str., Ia–IVa ip. def., as.
ν_{137}	B_{1g}	1434	–	273.2		CC str., I, III and II, IV oph.
ν_{136}	A_{1g}	1432	–	4741.4	1445 (R)	CC str., as., Kekule, Ia–IVa, COC ip. bend.
$\nu_{135(134)}$	E_u	1427	3.3	–		CC str., as., II, IV (I, III) iph.
$\nu_{133(132)}$	E_u	1412	125.0	–	1420 (IR)	CC str., as., Kekule, Ia, IIIa (IIa, IVa)
ν_{131}	B_{1g}	1378	–	142.8	1393 (R)	CC str., as., Kekule, Ia, IIIa and IIa, IVa oph.
ν_{130}	B_{2g}	1374	–	11.5		$C^{\beta}C^{\beta'}$ str. Ia–IVa def., as., CO str., s.
ν_{129}	A_{1g}	1361	–	4.7		CO str., s., CC str., as., Kekule, Ib–IVb iph., $C^{\alpha}C^{\beta}$, $C^{\alpha'}C^{\beta'}$ str., s.
$\nu_{128(127)}$	E_u	1351	27.1	–	1352 (IR)	CO str., s., CC str., as., Kekule, Ib, IIIb (IIb, IVb) oph.
$\nu_{125(124)}$	E_u	1334	19.0	–	1340 (IR)	CO str. as., CC str., as., I and III (II and IV) oph.
ν_{123}	B_{2g}	1333	–	548.1	1344 (R)	Ia–IVa, ip, def., as., CO str., s., $C^{\beta}C^{\beta'}$ str.
ν_{122}	B_{1g}	1312	–	863.5	1315 (R)	CC str., as., Kekule, Ib–IVb
$\nu_{121(120)}$	E_u	1292	5.8	–		CC str., as., Kekule, Ib, IIIb (IIb, IVb), CO str.
ν_{119}	A_{1g}	1286	–	851.4	1289 (R)	Ia–IVa and ct. bre., oph., CO str., CH ip. bend.
$\nu_{118(117)}$	E_u	1264	6.0	–	1268 (IR)	CH ip. bend., CO str., s., str. I, III (II, IV)
ν_{115}	B_{2g}	1237	–	54.6	1239 (R)	CH ip. bend.
ν_{114}	B_{1g}	1237	–	52.7	1239 (R)	Ia, IIIa and IIa, IVa, str., oph., CO str. as.
$\nu_{113(112)}$	E_u	1164	5.5	–	1172 (IR)	CH ip., bend., CO str., s.
ν_{111}	A_{1g}	1160	–	28.5		CH ip., bend., I–IV iph., CO str., s.
$\nu_{110(109)}$	E_u	1158	0.1	–		CH ip., bend.
ν_{108}	B_{1g}	1157	–	112.7	1160 (R)	CH ip., bend., CO str., as.
ν_{106}	B_{2g}	1135	–	0.4		CH ip., bend.
$\nu_{105(104)}$	E_u	1107	62.7	–	1102 (IR)	CO str., Ia, IIIa (IIa, IVa) ip. def., as., CH ip., bend.
ν_{103}	A_{1g}	1086	–	87.4	1087 (R)	Ia–IVa, ct. and fu. str., oph., CO str., s., COC ip. bend.
ν_{102}	B_{1g}	1073	–	3.5		CO str., as., CH ip. bend., I–IV str.
$\nu_{101(100)}$	E_u	1056	49.7	–		CO str., as., CH ip. bend., I–IV ip. def., s.
ν_{98}	A_{1g}	1024	–	19.7	1029 (R)	CH ip. bend., iph., CO str., s.
$\nu_{97(96)}$	E_u	1023	51.3	–	1024 (IR)	CO str., Ib–IVb., ip. def., as., CH ip. bend.
ν_{95}	B_{2g}	1018	–	0.9		Ib–IVb ip. def., as., CO str., s., fu str.
ν_{94}	B_{1g}	1018	–	19.8	1029 (R)	I, III and II, IV str., oph., CO str., as.
$\nu_{93(92)}$	E_u	995	16.1	–	1002 (IR)	Ib, IIIb (IIb, IVb) bre., oph., CO str., s.
$\nu_{90(89)}$	E_g	959	–	0.3		CH op. bend., as., II, IV (I, III)
ν_{87}	A_{1g}	933	–	1030.7	947 (R)	Ib–IVb and ct., fu. bre., oph., CH ip. bend.
ν_{86}	A_{2u}	927	2.8	–		CH op. bend., as., I, III and II, IV oph.
$\nu_{85(84)}$	E_g	926	–	0.1		CH op. bend., I, III (II, IV) oph.
$\nu_{81(80)}$	E_u	907	58.3	–	917 (IR)	I, III (II, IV) ip. sw., COC ip. bend.
ν_{79}	B_{2g}	903	–	17.1	913 (R)	I–IV ip. sw., COC ip. bend.
$\nu_{77(76)}$	E_g	853	–	7.3		CH op. bend., I, III (II, IV) iph.
$\nu_{73(72)}$	E_u	767	4.0	–		I, III (II, IV), fu. str., oph.
ν_{71}	A_{2u}	757	147.5	–	749 (IR)	CH op. bend., I–IV iph.
$\nu_{70(69)}$	E_g	754	–	3.0		CH op. bend., I, III (II, IV) oph.
$\nu_{66(65)}$	E_g	727	–	1.0		CH op. bend., I, III (II, IV) iph.
ν_{62}	B_{1g}	702	–	0.5		II, IV, ct. and I, III oph.
ν_{61}	B_{2g}	681	–	33.8	687 (R)	Ib–IVb ip. def., as.
$\nu_{60(59)}$	E_u	679	2.0	–	673 (IR)	fu. ip, sw., Ia, IIIa (IIa, IVa) def. as.
ν_{58}	A_{2u}	663	55.3	–	660 (IR)	CH, s., I–IV op. bend. and COC op. bend., iph.
$\nu_{57(56)}$	E_g	657	–	8.4		CH, COC op. bend.
ν_{53}	A_{1g}	644	–	21.3	651 (R)	Ib–IVb ip. def., s., iph.
$\nu_{52(51)}$	E_u	640	14.8	–		Ib and IIIb (IIb and IVb) ip. def., s., oph.
$\nu_{50(49)}$	E_g	640	–	0.8		Ia, IIIa (IIa, IVa), ct. op. def., iph.
ν_{47}	B_{1g}	554	–	24.3	559 (R)	I, III and II, IV ip. def., s., oph.
ν_{46}	A_{1g}	537	–	0.7		Ia–IVa, ct., fu. bre., iph.
$\nu_{45(44)}$	E_g	527	–	0.1		I, III (II, IV) op. def.
$\nu_{43(42)}$	E_u	524	1.8	–		I, III (II, IV) ip. def, as.; II, IV (I, III) ip. def. s

Table 3 (*Continued*)

Num.	Sym.	Fre.	I_{IR}	S_i	Exp.	Assignment
ν_{39}	B_{1g}	502	–	0.7	491 (R)	fu. sw., iph., Ia, IIIa and IIa, IVa ip. def., oph.
ν_{37}	B_{2g}	482	–	0.2		I–IV ip. def., as.
$\nu_{35(34)}$	E_g	466	–	0.1		I and III (II and IV) op. def., oph.
ν_{33}	A_{2u}	453	7.8	–		I–IV op. def., iph., CH op. bend.
$\nu_{32(31)}$	E_u	449	0.1	–		I and III (II and IV) ip. def., s., oph.
$\nu_{29(28)}$	E_g	395	–	1.5		I–IV op. def.
$\nu_{25(24)}$	E_u	328	1.1	–		II and IV (I and III) str. oph.
ν_{23}	A_{2u}	293	0.2	–		I, III and II, IV op. def., oph.
$\nu_{22(21)}$	E_g	285	–	1.3		I and III (II and IV) op. def., oph.
ν_{20}	A_{1g}	281	–	41.9	286 (R)	Skeleton bre., iph.
ν_{19}	B_{2g}	261	–	0.5	266 (R)	ct. ip. def., as.
$\nu_{18(17)}$	E_g	249	–	1.2		I–IV, fu. op. def.
ν_{15}	B_{1g}	213	–	32.0	218 (R)	ct. ip. def., s.
ν_{13}	A_{2u}	172	2.5	–		I–IV, ct and fu. op. def., oph.
$\nu_{11(10)}$	E_u	139	0.3	–		Ib, IIIb (IIb, IVb) ip. sw., iph.
$\nu_{9(8)}$	E_g	129	–	17.9	135 (R)	Ib, IIIb (IIb, IVb) waving, iph.
ν_6	B_{2g}	122	–	11.0	125 (R)	Ib–IVb sw.
$\nu_{5(4)}$	E_g	72	–	2.3	61 (R)	Skeleton op. waving
ν_2	A_{2u}	36	0.9	–		Skeleton waving

No., mode number; Sym., symmetry species; Fre., frequency (cm^{-1}); I_{IR}, IR intensity (km/mol); S_i, Raman activity ($Å^4$/amu); Exp., experimental; def., deformation; bre., breathing; s., symmetric; as., asymmetric; iph., in-phase; oph., out-of-phase; I, II, III, IV, benzene ring numbers (see Fig. 2); bend., bending; sw., swinging; fu., furan; ct., cyclooctateraene ring, str., stretching; ip., in-plane; op., out-of-plane.

The naphthalene A_g ν_{33} mode (which belongs to the Kekule vibrations) produces in Raman spectrum of 4N the modes B_{1g} ν_{131} and A_{1g} ν_{136} of the Kekule vibrations in the "a" naphthalene rings and also similar modes B_{1g} ν_{122} and A_{1g} ν_{129} in the "b" rings. Besides this, the observed Raman band at 1289 (A_{1g} ν_{119}) also has contributions of the Kekule vibrations in the "b" naphthalene rings.

4.3.2.2. Furan related vibrations. The symmetric CC bond vibrations of the free furan molecule (A_1: calc. ν_{16} = 1483 cm^{-1}) in the Raman spectrum of the 4N species are mixed with the ν(CC) vibrations of naphthalene rings; being calculated at 1465 cm^{-1} they provide an intense Raman line 1468 cm^{-1} (ν_{147}, Table 3).

Vibrations of the CO bonds in IR spectrum of 4N are calculated in the range 1351–995 cm^{-1}. In the high-frequency region (1351–1292 cm^{-1}) they are mixed with the ν_{as}(CC) vibrations of the naphthalene rings ($\nu_{128(127)}$, $\nu_{125(124)}$, $\nu_{121(120)}$); at lower frequencies they are mixed with δ(CH) deformation vibrations (symmetric and asymmetric) of naphthalene fragments ($\nu_{118(117)}$, $\nu_{113(112)}$, $\nu_{105(104)}$, $\nu_{101(100)}$). These are doubly degenerate vibrations of the E_u symmetry, which are formed upon combination of the respective furan vibrations of the A_1 and B_2 symmetry (Table 1); in the observed IR spectrum of 4N these vibrations produce absorption bands in the whole frequency region from 1352 till 1002 cm^{-1}. The furan vibrations of the A_1 and B_2 symmetry in Raman spectrum of 4N (D_{4h} point group) transform into the A_{1g}, B_{1g}, A_{2g}, B_{2g} symmetries and are mixed with those types of vibrations which are described in the IR spectrum of 4N in the range 1374–1018 cm^{-1}.

4.3.2.3. Deformation vibrations of the rings. The planar skeleton deformation in the IR spectrum of 4N are calculated at 1264 cm^{-1} (exp.: 1268 cm^{-1}), 1107 cm^{-1} (exp.: 1102 cm^{-1}), 1023 cm^{-1} (exp.: 1024 cm^{-1}), 995 cm^{-1} (exp.: 1002 cm^{-1}), 907 cm^{-1} (exp.: 917 cm^{-1}), 679 cm^{-1} (exp.: 673 cm^{-1}). These modes consist of symmetric and asymmetric deformations, breathing of rings and are mixed with δ(CH), ν(CO) or COC angles deformation. In the Raman spectrum of 4N the most active planar skeleton deformation is the totally symmetric A_{1g} mode ν_{87} (calc.: 933 cm^{-1}, exp.: 947 cm^{-1}), which belongs to the in-phase breathing deformation of the Ib–IVb rings being out-of-phase to the furan and eight-member ring breathings. For comparison, in the naphthalene Raman spectrum the breathing vibration is calculated at 752 cm^{-1} (A_g ν_{12}), in the furan molecule – at 860 cm^{-1} (A_1 ν_7). The cyclooctatetraene ring breathing vibration, calculated in our DFT approach at 537 cm^{-1} (A_g ν_{46}), provides low activity in the Raman spectrum of 4N.

In low frequency region the most active mode is A_{1g} ν_{20} (calc.: 281 cm^{-1}, exp.: 286 cm^{-1}), which belongs to breathing vibration of the whole skeleton of the 4N molecule, and the B_{1g} ν_{15} (calc.: 213 cm^{-1}, exp.: 218 cm^{-1}), determining symmetric deformations of the eight-member ring. The corresponding asymmetric deformations of the ring (B_{2g} ν_{19}) are low active in Raman scattering.

The out-of-plane deformations of the rings (ν_{23}, ν_{13}) of the A_{2u} symmetry, which are allowed in the IR spectrum of 4N, and the corresponding E_g deformations, allowed in Raman spectrum, exhibit low activity. Among the latter modes we can specify the waving vibration of two opposite-lying naphthalene rings $\nu_{9(8)}$ (calc.: 129 cm^{-1}), which shows relatively high Raman activity (17.9 $Å^4$/amu). The out-of-plane skeleton deformations of the B_{2u}, A_{1u}, B_{1u} symmetry are forbidden in both (IR and Raman) spectra.

5. Conclusions

We have presented experimental FTIR and Raman spectra of two symmetric derivatives of the tetraoxa[8]circulenes which have been interpreted by the density functional theory (DFT). The tetraphenylenotetrafuran (4B) and tetranaphthylenotetrafuran (4N) molecules which belong to the D_{4h} symmetry point group have been studied and their equilibrium molecular structures, harmonic vibrational frequencies, IR absorption intensities and Raman scattering activities have been calculated by the DFT/B3LYP method with the 6–31G(d) basis set using the D_{4h} symmetry constrains. All 102 normal modes of 4B and 174 modes of the 4N molecule are calculated and analyzed (many of them are degenerate). Spectroscopically active 81 modes of 4B (38 IR, 43 R) and 138 active modes of 4N (65 IR, 73 R) are presented in Tables 2 and 3 with a complete assignment of their structural nature. In order to classify vibrational origins of the tetraoxa[8]circulene modes we have compared them with the calculated modes and the IR and Raman spectra of the benzene, naphthalene and furan. Some forbidden modes of these fragments are allowed in the tetraoxa[8]circulenes, which is observed in the spectra.

Correlation diagrams with symmetry account of vibrational modes in the studied molecules and their constituents (benzene, naphthalene and furan) have proven very useful in the force field and frequency analysis. Comparison of the calculated vibrational spectra with the experimental data provides very reliable

assignments of all observed bands in FTIR and Raman spectra of the tetraoxa[8]circulenes and help in additional interpretation of some forbidden modes of the constituent molecules. The corresponding small frequency shifts are well reproduced. The reference spectra also help in the assignment of the close lying bands from different fragments, which almost coincide in the observed spectra. In the experimental detection we observe even very weak IR bands with the calculated intensity up to 1–2 km/mole (supplementary material). In the Raman spectra we have interpreted all bands including the low frequency region (up to 61 cm^{-1} in 4N). The detailed analysis of all bands is necessary from the point of fundamental importance of these highly symmetric tetraoxa[8]circulenes vibration assignment.

Appendix A. Supplementary data

Supplementary data associated with this article can be found, in the online version, at doi:10.1016/j.vibspec.2012.02.005.

References

[1] C.B. Nielsen, T. Brock-Nannestad, T.K. Reenberg, P. Hammershøj, J.B. Christensen, J.W. Stouwdam, M. Pittelkow, Chem. Eur. J. 16 (2010) 13030–13034.
[2] J. Eskildsen, T. Reenberg, J.B. Christensen, Eur. J. Org. Chem. 2000 (2000) 1637–1640.
[3] B.F. Minaev, G.V. Baryshnikov, V.A. Minaeva, Comput. Theor. Chem. 972 (2011) 68–74.
[4] J. Eskildsen, P. Hammershшj, T.K. Reenberg, U. Larsen, M. Pittelkow, S.M. Leth, R.A. Peck, J.B. Christensen, Asian Chem. Lett. 11 (2007) 211–218.
[5] K. Yu Chernichenko, E.S. Balenkova, V.G. Nenajdenko, Mendeleev Commun. 18 (2008) 171–179.
[6] T. Brock-Nannestad, C.B. Nielsen, M. Schau-Magnussen, P. Hammershøj, T.K. Reenberg, A.B. Petersen, D. Trpcevski, M. Pittelkow, Eur. J. Org. Chem. 2011 (2011) 6320–6325.
[7] I. Perepichka, D. Perepichka, H. Meng, F. Wudlt, Adv. Mater. 17 (2005) 2281–2305.
[8] R. Rathore, S.H. Abdelwahed, Tetrahedron Lett. 45 (2004) 5267–5270.
[9] H. Erdtman, H.E. Högberg, Chem. Commun. (1968) 773–774.
[10] H. Erdtman, H.E. Högberg, Tetrahedron Lett. 11 (1970) 3389–3392.
[11] H.E. Högberg, Acta Chem. Scand. 26 (1972) 309–316.
[12] H.E. Högberg, Acta Chem. Scand. 26 (1972) 2752–2758.
[13] H.E. Högberg, Acta Chem. Scand. 27 (1973) 2559–2566.
[14] H.E. Högberg, Acta Chem. Scand. 27 (1973) 2591–2596.
[15] J.-E. Berg, H. Erdtman, H.E. Högberg, B. Karlsson, A.-M. Pilotti, A.-C. Söderholm, Tetrahedron Lett. 18 (1977) 1831–1834.
[16] T. Liljefors, O. Wennerström, Tetrahedron 33 (1977) 2999–3003.
[17] R. Salcedo, L.E. Sansores, A. Picazo, L. Sansyn, J. Mol. Struct.: Theochem. 678 (2004) 211–215.
[18] K.Yu. Chernichenko, V.V. Sumerin, R.V. Shpanchenko, E.S. Balenkova, V.G. Nenajdenko, Angew. Chem. Int. Ed. 45 (2006) 7367–7370.
[19] T. Fujimoto, R. Suizu, H. Yoshikawa, Awaga Chem. Eur. J. 14 (2008) 6053–6056.
[20] T. Fujimoto, M.M. Matsushita, H. Yoshikawa, K. Awaga, J. Am. Chem. Soc. 130 (2008) 15790–15791.
[21] S. Mohakud, S.K. Pati, J. Mater. Chem. 19 (2009) 4356–4361.
[22] S.S. Bukalov, L.A. Leites, K.A. Lyssenko, R.R. Aysin, A.A. Korlyukov, J.V. Zubavichus, K.Yu. Chernichenko, E.S. Balenkova, V.G. Nenajdenko, M.Yu. Antipin, J. Phys. Chem. A 112 (2008) 10949–10961.
[23] G. Gahungu, J. Zhang, Phys. Chem. Chem. Phys. 10 (2008) 1743–1747.
[24] G. Gahungu, J. Zhang, T. Barancira, Phys. Chem. J. A 113 (2009) 255–262.
[25] A. Dadvand, F. Cicoira, K.Yu. Chernichenko, E.S. Balenkova, R.M. Osuna, F. Rosei, V.G. Nenajdenko, D.F. Perepichka, Chem. Commun. (2008) 5354–5356.
[26] O. Ivasenko, J.M. MacLeod, K.Yu. Chernichenko, E.S. Balenkova, R.V. Shpanchenko, V.G. Nenajdenko, F. Rosei, D.F. Perepichka, Chem. Commun. (2009) 1192–1194.
[27] B. Napolion, F. Hagelberg, M.-J. Huang, J.D. Watts, T.M. Simeon, D. Vereen, W.L. Walters, Q.L. Williams, Phys. Chem. J. A 115 (2011) 8682–8690.
[28] A.D. Becke, J. Chem. Phys. 7 (1993) 5648–5652.
[29] C. Lee, W. Yang, R.G. Parr, Phys. Rev. B 37 (1988) 785–789.
[30] M.M. Francl, W.J. Petro, W.J. Hehre, J.S. Binkley, M.S. Gordon, D.J. DeFrees, J.A. Pople, J. Chem. Phys. 77 (1982) 3654–3666.
[31] M. Frisch, G. Trucks, H. Schlegel, G. Scuseria, M. Robb, J. Cheeseman, J. Montgomery, J. Vreven, K. Kudin, J. Burant, J. Millam, S. Iyengar, J. Tomasi, V. Barone, B. Mennucci, M. Cossi, G. Scalmani, N. Rega, G. Petersson, H. Nakatsuji, M. Hada, M. Ehara, K. Toyota, Fukuda, J. Hasegawa, M. Ishida, T. Nakajima, Y. Honda, O. Kitao, H. Nakai, M. Klene, X. Li, R.J. Knox, H. Hratchian, J. Cross, V. Bakken, C. Adamo, J. Jaramillo, R. Gomperts, R. Stratmann, O. Yazyev, A. Austin, R. Cammi, C. Pomelli, J. Ochterski, P. Ayala, K. Morokuma, G. Voth, P. Salvador, J. Dannenberg, V. Zakrzewski, S. Dapprich, A. Daniels, M. Strain, O. Farkas, D. Malick, A. Rabuck, K. Raghavachari, J. Foresman, J. Ortiz, Q. Cui, A. Baboul, S. Clifford, J. Cioslowski, B. Stefanov, G. Liu, A. Liashenko, P. Piskorz, I. Komaromi, R. Martin, D. Fox, T. Keith, M. Al-Laham, C. Peng, A. Nanayakkara, M. Challacombe, P. Gill, B. Johnson, W. Chen, M. Wong, C. Gonzalez, J. Pople, Gaussian 03, Revision C.02, Gaussian, Inc., Wallingford, CT, 2004.
[32] A.P. Scott, L. Radom, J. Phys. Chem. 100 (1996) 16502–16513.
[33] P.L. Polavarapu, J. Phys. Chem. 94 (1990) 8106–8112.
[34] G. Keresztury, S. Holly, G. Besenyei, J. Varga, A. Wang, J.R. Durig, Spectrochim. Acta 49 (1993) 2007–2026.
[35] S.I. Gorelsky, SWizard Program, University of Ottawa, Ottawa, Canada, 2010. http://www.sg-chem.net/.
[36] L.J. Bellamy, The Infra-Red Spectra of Complexes Molecules, Methuen & Co. Ltd., London, UK, 1954.
[37] G. Socrates, Infrared Raman Characteristic Group Frequencies – Tables and Charts, 3rd ed., J. Wiley & Sons, Chichester, 2001.
[38] L. Goodman, A.G. Ozkabak, S.N. Thakur, J. Phys. Chem. 95 (1991) 9044–9058.
[39] The official web site of National Institute of Advanced Industrial Science and Technology (AIST), Research Information Database (RIO-DB). http://riodb.ibase.aist.go.jp/riohomee.html.
[40] E.B. Wilson, Phys. Rev. 45 (1934) 706–714.